

# Super-resolution of Wind Data and Compressed Utilization for Atmospheric Dispersion Modeling near Nuclear Power Plants: Based on Deep Learning and SVD

Dakyoung Lee, Juryong Park\*, Eung Soo Kim\*  
Department of Nuclear Engineering, Seoul National University  
E-mail: itts9904@snu.ac.kr, kes7741@snu.ac.kr

## 1. Introduction

When radioactive substances are released into the atmosphere in the vicinity of a nuclear power plant, various physical, chemical, and biological transport processes, as well as dispersion and deposition processes, occur depending on meteorological conditions and topography, leading to the redistribution of concentrations. Particularly, local wind conditions have a significant impact on dispersion, making predictions complex due to diverse local winds and seasonal meteorological changes around nuclear power plants. Therefore, for accurate atmospheric dispersion predictions, it is necessary to utilize 3D meteorological models and atmospheric dispersion models, considering wind fields and emission conditions.

To rapidly and accurately calculate the dispersion of radioactive materials, obtaining high-resolution wind information over a spatially confined area to precisely understand wind characteristics is crucial. However, as meteorological data becomes higher in resolution, the data volume exponentially increases, potentially causing data overload issues. Thus, efficient data compression methods are needed to apply large-scale high-resolution wind data to atmospheric dispersion models.

In this study, we introduce an algorithm that combines Deep learning for generating high-resolution wind data and data compression using SVD to efficiently apply high-resolution wind data to atmospheric dispersion models. Specifically, we targeted the Kori Nuclear Power Plant, which has the highest population density near a domestic nuclear power plant, and extracted high-resolution wind speed data ( $U$ ,  $V$ ) using WRF for the year 2022, twice a day (12 am, 12 pm). This data was then utilized as a dataset for Deep learning training, and the process involves applying SVD decomposition to the output high-resolution wind data to compress the data.

## 2. Methodology

### 2.1 Constructing Datasets using WRF

The mesoscale numerical weather prediction model WRF-ARW (Advanced Research WRF) v4.1 was used to obtain high-resolution wind data in the vicinity of the Kori NPP [1]. WRF is a community model developed around the National Center for Atmospheric Research (NCAR) in the United States that uses the Arakawa-C horizontal grid scheme to simulate compressible, non-stationary atmospheric flow fields. The modeling domain is constructed using a nesting technique,

comprising the first domain covering the Korean Peninsula with a grid resolution of 1.5 km and the final analysis domain, focusing on the Kori Nuclear Power Plant area, with a horizontal resolution of 300 m (Figure 1). The vertical layers consist of a total of 23 levels, mirroring the vertical levels of LDAPS (Local Data Assimilation and Prediction System), which are defined as (pressure levels (hPa): 1000, 975, 950, 925, 900, 875, 850, 800, 750, 700, 650, 600, 550, 500, 450, 400, 350, 300, 250, 200, 150, 100, 70).

The initial and boundary data for the WRF model were obtained from the LDAPS regional forecasting model provided by KMA (Korea Meteorological Administration), which offers 3-hourly interval data at a 1.5 km grid resolution.

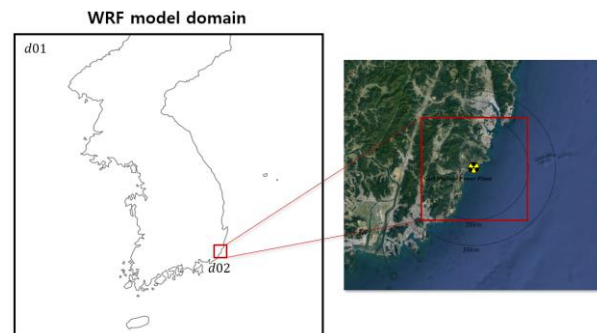


Fig. 1. Setting up domains for high-resolution simulation near the Kori Nuclear Power Plant using WRF.

### 2.2 Uformer Model

Image restoration aims to recover high-quality images from their degraded counterparts and encompasses a range of computer vision applications such as image super-resolution (SR) and noise reduction. Recently, Transformer-based image restoration networks have showcased promising advancements over convolutional neural networks, thanks to their parameter-independent global interactions [2]. The fusion of Transformer and UNet architectures in Uformer empowers it with the capability to capture both local and global dependencies for image restoration tasks. In this study, we leverage the Transformer-based Uformer model for the enhancement of meteorological data through deblur.

LDAPS data was assumed to be a blurred version of WRF data, and the Uformer model's deblurring function was employed to produce data with more physically accurate characteristics. To use the Uformer model, a preprocessing step was undertaken to upscale LDAPS data to the size of WRF data, resulting in the creation of

128x128 data by filling in duplicate values. In this paper, we refer to the process of using this duplicated 128x128 LDAPS data as input and WRF data as the target output to increase the number of meaningful pixels as 'Super-resolution'.

The structure of the Uformer is shown in Figure. 2. Uformer is based on UNet [3] architecture, where modifying the convolution layers to Transformer blocks while keeping the same overall hierarchical encoder-decoder structure and the skip-connections [4]. Unlike traditional ConvNet-based architectures, Uformer is built upon the LeWin Transformer block, a crucial component that allows it to not only handle local context but also efficiently capture long-range dependencies.

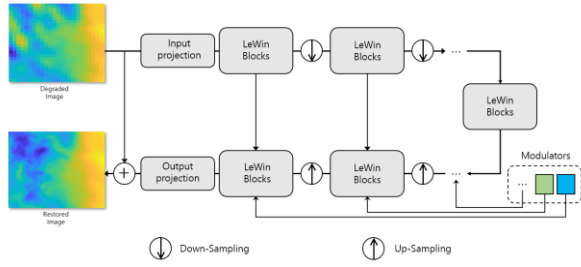


Fig. 2. Overview of Uformer

### 2.3 SVD for Data Compression

SVD with the maximum energy packing property is usually used in compression. SVD decomposes a matrix into orthogonal components with which optimal sub-rank approximations may be obtained [5]. As illustrated in equation (1), truncated SVD transformation with rank  $r$  may offer significant savings in storage over storing the whole matrix with accepted quality.

$$X = \sum_{i=1}^k S_i U_i V_i^T \approx s_1 u_1 v_1^T + s_2 u_2 v_2^T + \dots + s_k u_k v_k^T \quad (1)$$

Where  $R$  is the compression percentage,  $k$  is the chosen rank for truncation;  $m$  and  $n$  are the number of rows and columns in the image respectively.

$$R = \frac{nk+k+mk}{nm} * 100 \quad (2)$$

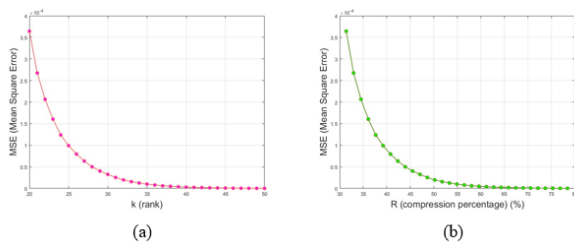


Fig. 3. (a) Change in MSE with Compression Ratio R (b) Change in MSE with Rank R

In this study, SVD decomposition was performed at  $k=43$  and  $R=67.4500$  in consideration of the compression efficiency of wind data according to Figure. 3., and data compression was achieved at a scale of 1/3 of the original data.

### 2.4 Lagrangian Particle Dispersion Model (LPDM)

The atmospheric dispersion model can be broadly categorized into Lagrangian and Eulerian methods. The Lagrangian method has the advantage of convenient treatment of point sources compared to the Eulerian method. In the case of a nuclear power plant accident, the atmospheric dispersion and transport of radioactive isotopes involve treating point sources, making the Lagrangian method more useful than the Eulerian method for calculating the spread of radioactive materials. Therefore, this study employed the Lagrangian particle dispersion model as the atmospheric dispersion model for conducting the research.

Among Lagrangian methods, the Lagrangian Particle Dispersion Model (LPDM) represents atmospheric pollution as particles are continuously emitted. It determines the positions of each emitted particle as follows:

The movement of particles within the flow is represented by Equation (3).

$$\frac{dX}{dt} = U \quad (3)$$

$X$  represents the spatial position of particles, and  $U$ , the wind component at the particle's location, is expressed as Equation (4).

$$U = \bar{U} + U_t \quad (4)$$

The particle velocity  $\bar{U}$  represents the average velocity of particles influenced by meteorological data, while  $U_t$  corresponds to the fluctuation attributed to turbulence effects.

Turbulence induces small displacements in fluid motion, and these small displacements possess a random nature. The turbulent component in the horizontal direction is calculated as shown in Equations (5) and (6).

$$u_t(t + dt) = u_t(t) + du_t(t) \quad (5-a)$$

$$v_t(t + dt) = v_t(t) + dv_t(t) \quad (5-b)$$

$$du_t(t) = -u_t(t) \frac{dt}{T_{Lu}} + \sqrt{\frac{2dt}{T_{Lu}}} \sigma_{us} \text{RAND}(0,1) \quad (6-a)$$

$$dv_t(t) = -v_t(t) \frac{dt}{T_{Lv}} + \sqrt{\frac{2dt}{T_{Lv}}} \sigma_{vs} \text{RAND}(0,1) \quad (6-b)$$

$T_{Lu}$  and  $T_{Lv}$  represent the Lagrangian time scales, while  $\sigma_{us} \text{RAND}(0,1)$  and  $\sigma_{vs} \text{RAND}(0,1)$  denote random numbers from a normal distribution with mean 0 and standard deviation  $\sigma_{us}$  and  $\sigma_{vs}$ , respectively,

representing the random standard deviations of turbulent velocity components.

### 3. Results and Discussion

#### 3.1 Error Analysis of Wind Data Super-Resolution using Uformer

In this study, a model is trained to generate high-resolution (300 m) data using the 1.5 km LDPAS model input from the Korea Meteorological Administration. For training, a dataset was constructed by collecting data from January to December 2022. For testing, random samples from January, March, and May 2023, spanning 1 to 5 days each, were used. The wind vector elements U and V were used as the training features.

Figure. 4. visualizes the test results of the Uformer model, comparing the generated output with the input LDAPS data and the target WRF data. The results generated by Uformer exhibit a higher resolution than the input LDAPS data, and overall show similar analysis patterns to manually generated high-resolution WRF analysis data.

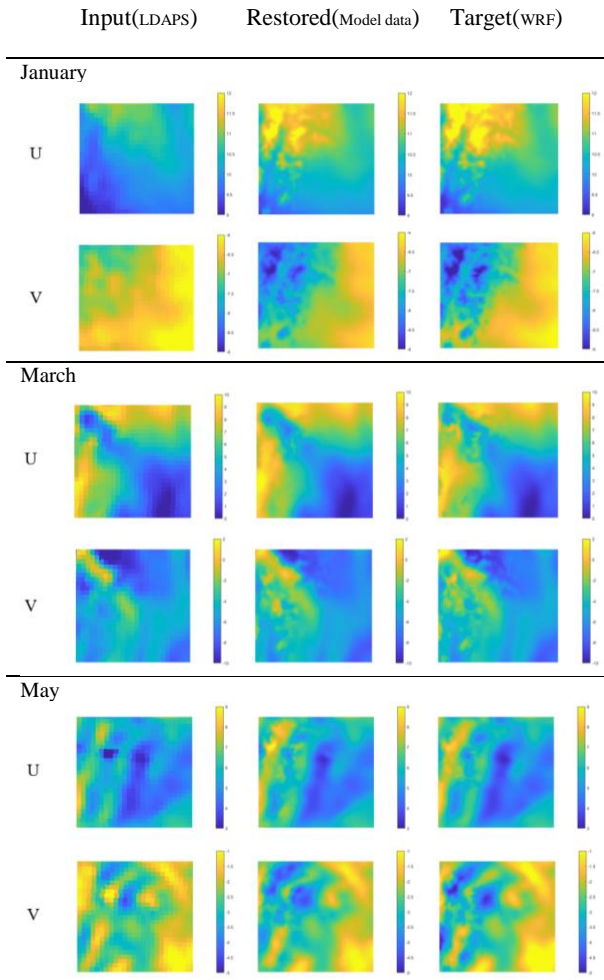


Fig. 4. Visual evaluation of generated high-resolution analysis data, LDAPS model data, and WRF performance results

	PSNR (dB)	SSIM	R-squared
Jan U	31.984	0.972	0.961
Jan V	28.751	0.957	0.930
Mar U	24.467	0.901	0.955
Mar V	27.152	0.944	0.938
May U	23.156	0.925	0.949
May V	23.283	0.920	0.909

Table. 1. Quantitative evaluation of Uformer using PSNR, SSIM, and R-squared

Table. 1. presents the evaluation results of the Uformer model's test outcomes depicted in Figure. 4., measuring PSNR, SSIM, and R-squared between the model data and the WRF analysis data. PSNR (Peak Signal-to-Noise Ratio) is one of the quantification methods for assessing the quality loss of restored images, while SSIM (Structural Similarity Index) measures the structural similarity index between distortion-free high-quality images and restored images. As the high-resolution wind data generated through Uformer becomes more similar to manually generated high-resolution WRF analysis data, both PSNR and SSIM show improvement. Furthermore, R-squared was utilized to evaluate the predictive performance of the model. Among the random test results, the highest and lowest PSNR values are 31.984 and 23.156, respectively. The results of SSIM and R-squared demonstrate values exceeding 0.9 for the U and V test datasets of January, March, and May, confirming that the model data closely predicts WRF's high-resolution analysis data.

Furthermore, utilizing Uformer for high-resolution wind data prediction offers temporal efficiency compared to high-resolution wind data prediction through WRF. While manually generating high-resolution analysis data using the CPU (Intel Core i5-9600K CPU, 3.70GHz) might take at least several tens of minutes, using Uformer based on the GPU (NVIDIA GeForce RTX 3090) takes only about 0.276 seconds for high-resolution enhancement.

In this manner, the creation of high-resolution wind data through the Uformer model offers the advantage of producing similar high-resolution data as generated by WRF, while also providing the convenience of obtaining it much more quickly within a simplified timeframe.

#### 3.2 Lightweight Compression of Wind Data

The model data obtained through Uformer, i.e., the restored data, is in a resolution of 300m, which results in an approximately 25 times increase in data volume compared to the LDAPS model data with a resolution of 1.5km. Such a significant increase in data volume can hinder the efficient utilization of high-resolution wind data. Therefore, in this study, we aim to address the issue of capacity overload caused by high resolution by



employing SVD compression on the model data, which is then used in atmospheric dispersion models.

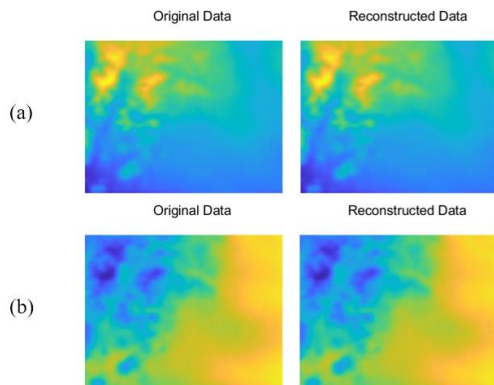


Fig. 5. SVD Based Compression (a) Comparison of January U-wind data between original data and compression ratio 67% (truncation to  $k=43$ ). (b) Comparison of January V-wind data between original data and compression ratio 67% (truncation to  $k=43$ ).

As shown in Figure 5, when data compression was performed at a compression ratio of 67% through SVD decomposition, the MSEs of the original data and the reconstruction data were (a)  $3.2823e-06$  and (b)  $4.5704e-06$ , respectively. Therefore, through Singular Value Decomposition (SVD), we have been able to obtain results very similar to using the entire original data by utilizing only 67% of the original data.

### 3.3 Results of the Lagrangian Particle Dispersion Model Execution

We conducted numerical simulations using the Lagrangian Particle Dispersion Model (LPDM) on high-resolution wind data (U, V) generated through Uformer after compressing the data using Singular Value Decomposition (SVD).

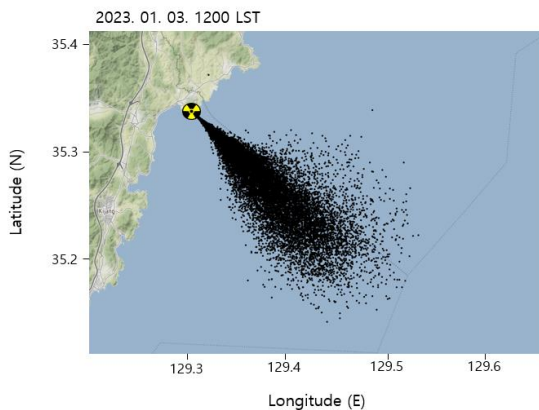


Fig. 6. Horizontal distributions simulated for one hour using LPDM at 1200 LST on January 3, 2023, from the Kori Nuclear Power Plant.

Figure. 6. shows the results of performing Lagrangian Particle Dispersion (LPDM). The hypothetical release point of particles was set to 129.3E, 35.3N, corresponding to the location of the Kori Nuclear Power Plant. The model was executed to simulate particle dispersion at 700 hPa over a duration of one hour with constant particle emission.

Thus, we have demonstrated that the high-resolution wind data rapidly obtained through Uformer can effectively be applied to LPDM using only 67% of the data through SVD.

## 4. Conclusions

This study introduces an algorithm that applies Deep learning and SVD decomposition to wind data, enabling a precise understanding of wind characteristics while achieving high compression efficiency. Although the study covers only an area of approximately 1470 km<sup>2</sup> based on the Kori Nuclear Power Plant, not encompassing the entire Korean Peninsula, and primarily focuses on increased horizontal resolution, it provides valuable insights that can contribute to more accurate and efficient atmospheric dispersion modeling results.

## Acknowledgement

This work was supported by the Nuclear Safety Research Program through the Korea Foundation Of Nuclear Safety(KoFONS) using the financial resource granted by the Nuclear Safety and Security Commission(NSSC) of the Republic of Korea. (No. 2105010-0222-WT112)

## REFERENCES

- [1] Skamarock, W. C., Klemp, J. B., Dudhia, J., Gill, D. O., Liu, Z., Berner, J., ... Huang, X. -yu. (2019). A Description of the Advanced Research WRF Model Version 4.1 (No. NCAR/TN-556+STR). doi:10.5065/1dfh-6p97.
- [2] Zhang, J., Zhang, Y., Gu, J., Zhang, Y., Kong, L., & Yuan, X. (2022). Accurate image restoration with attention retractable transformer. arXiv preprint arXiv:2210.01427.
- [3] Ronneberger, O., Fischer, P., & Brox, T. (2015). U-net: Convolutional networks for biomedical image segmentation. In Medical Image Computing and Computer-Assisted Intervention–MICCAI 2015: 18th International Conference, Munich, Germany, October 5-9, 2015, Proceedings, Part III 18 (pp. 234-241). Springer International Publishing.
- [4] Wang, Z., Cun, X., Bao, J., Zhou, W., Liu, J., & Li, H. (2022). Uformer: A general u-shaped transformer for image restoration. In Proceedings of the IEEE/CVF conference on computer vision and pattern recognition (pp. 17683-17693).
- [5] Sadek, R. A. (2012). SVD based image processing applications: state of the art, contributions and research challenges. arXiv preprint arXiv:1211.7102.